Extracting ultralight boson properties from boson clouds around postmerger remnants

Kelvin H. M. Chan* and Otto A. Hannuksela†

Department of Physics, The Chinese University of Hong Kong, Shatin, New Territories, Hong Kong

(Received 29 January 2023; accepted 24 October 2023; published 5 January 2024)

Ultralight bosons are a class of hypothetical particles that could potentially solve critical problems in fields ranging from cosmology to astrophysics and fundamental physics. If ultralight bosons exist, they form clouds around spinning black holes with sizes comparable to their particle Compton wavelength through superradiance. This well-understood classical wave amplification process has been studied for decades. After these clouds form, they dissipate and emit continuous gravitational waves through the annihilation of ultralight bosons into gravitons. These gravitons could be detected with ground-based gravitational-wave detectors using continuous-wave searches. However, it is conceivable for other continuous-wave sources to mimic the emission from the clouds, which could lead to false detections. Here, we investigate how to use continuous waves from clouds formed around known merger remnants to alleviate this problem. In particular, we simulate a catalog of merger remnants that form clouds around them and demonstrate with select "golden" merger remnants how one can perform a Bayesian cross-verification of the ultralight boson hypothesis that has the potential to rule out alternative explanations. Our proof-of-concept study suggests that, in the future, there is a possibility that a merger remnant exists close enough for us to perform the analysis and test the boson hypothesis if the bosons exist in the relevant mass range. Future research will focus on building more sophisticated continuous-wave tools to perform this analysis in practice.

DOI: 10.1103/PhysRevD.109.023009

I. INTRODUCTION

Ultralight bosons (ULBs) are a broad class of hypothetical integer spin particles with mass $\ll 1$ eV [1–3], including axionlike particles [4,5], dilatons [6], and Majorons [7]. They have been promising dark matter (DM) candidates [8–14] and solutions to various problems in particle physics, astrophysics, and cosmology [6,8,15–23].

If ULBs exist in nature, they will couple to rotating black holes with Schwarzschild radii similar to the boson's Compton wavelength through a process called superradiant instability, forming clouds of boson particles [16,24]. In particular, when a superradiant instability is spontaneously triggered, the boson fields around a rotating black hole (BH) will extract energy and angular momentum of the host BH to create bosons around the BH [24–30]. The process continues to spin down the host BH and extract its mass and angular momentum until the rotational frequency of the black hole matches approximately the boson Compton frequency [24].

It is particularly interesting that the formation of such a bosonic cloud could lead to potentially observable signatures. In particular, when the cloud reaches a macroscopic size, it can emit continuous quasimonochromatic gravitational waves (GWs) through the annihilation of bosons into gravitons [18,28,31–35]. Furthermore, because the superradiance effect spins down rotating black holes, another observational signature is a dearth of rotating black holes above the expected critical spin set by the boson mass (so-called Regge trajectory) [24]. Also, it is possible to observe a time evolution of the supermassive black hole shadow [36,37]. Finally, it is also possible for the presence of the cloud to disturb binary orbits [38–46] and, under specific scenarios, couple to magnetic fields and emit photons [47,48] or explode in a "bosenova" due to self-interactions [24,49].[1] Indeed, a wide range of observational signatures is possible.

Scientists can now utilize a wide range of astrophysical messengers, including the wide spectrum of electromagnetic waves, cosmic rays, and neutrinos in the hunt for beyond-standard-model particles. In recent years, gravitational-wave observations have also become commonplace [51]. With the advent of these new gravitational observations, scientists can now perform searches for

*kelvinhmchan@link.cuhk.edu.hk
†otto.akseli.hannuksela@gmail.com

[1]Note that the mechanism behind the scalar version of the bosenova in the nonrelativistic regime has been discussed in the recent literature [50].

DM candidates like primordial black holes and ULBs using GWs in addition to the existing messengers [52–55].

In particular, several efforts search for these ultralight bosons using table-top experiments or astronomical observations [17,29,31,33,34,40,56–81]. Spin measurements of BHs in x-ray binaries (see [82,83]) could be used to search for bosons in the mass ranges of $5M_\odot < M \lesssim 20M_\odot$ [82,84]. Gravitational-wave observations of black hole spin from binary black hole coalescences provide another avenue, as they encode the properties of their sources, including the masses and spins of the two-component BHs, which could allow us to observe the dearth of high-spin black holes predicted by the existence of the ULBs [32,81,85]. Since ground-based GW detectors can detect heavier BHs (M up to $\sim 100M_\odot$) [51,86,87] than those found in x-ray binaries, the spin measurements inferred from GWs probe a lighter range of boson mass. Another major, related area is to study signatures in the observations of gravitational waveforms during binary coalescence [39,88–91]. When a large number of black hole/cloud systems are present, stochastic GW can also probe the presence of ULBs [32,34]. Finally, existing searches also include directed searches and all-sky searches for continuous gravitational waves (CWs). These CW searches employ semicoherent methods such as the Hidden Markov Model (HMM), in which the full-length data are broken into smaller chunks of data to analyze coherently [28,53,69,75] (see [92] for a review on CW searches).

However, there are certain known limitations to the existing searches. For example, searching for holes in the Regge plane requires the timescale between the formation of BHs and the merger to be larger than the superradiant timescale for the ULB cloud to form and spin down the BH [32,81,85], and the formation or presence of the clouds could in theory be tidally disrupted [41,44]. In addition, searching for the CW signals from ULB clouds may be difficult as the other CW sources could in principle mimic the GWs from a ULB cloud.

One way to reduce the probability of false detections in CW searches is with directed searches targeting known merger remnants [28,29,31,67,70,76]. By analyzing the merger waveform, we know the sky position of any observed merger remnant, and therefore a directed search would both allow us to reduce the background noise and also link the CW signal to the merger remnant, reducing the probability that the signal originated from another source [28,70,76]. In this work, we demonstrate how the remnant BH's properties can, in addition, be used in the analysis to further reduce the probability of false detections.

In this work, we focus on scalar (spin-0) and vector (spin-1) bosons, where the physics is well studied [18,24,27–29,32,39,93–95]. Meanwhile, theoretical studies on tensor (spin-2) bosons [30,96] have yet to include a comprehensive calculation of gravitational-wave emissions.

The paper is structured as follows. In Sec. II, we review the physics of the ULB clouds formed around rotating BHs and the GW emission. We then discuss how focusing on clouds around merger remnants may aid the searches for ULBs. In Sec. III, we use the standard signal-to-noise (SNR) calculations in gravitational-wave physics to evaluate the detection horizon of clouds formed around merger remnants by different GW observatories. We then compare the horizon with the existing forecast on merger events. In Sec. IV, we perform a mock analysis with a "golden" remnant from the merger forecast catalog, to show that by obtaining a coherent boson cloud measurement we can cross-verify the existence of ULBs. Finally, we conclude in Sec. V.

II. BOSON CLOUD

In this section, we review the physics of boson fields around rotating BHs in a manner that is best suited for the later discussion. We first review the formation of the macroscopic boson cloud, and then the gravitational waves emission by the cloud.

A. Cloud formation

For a Kerr BH [97] of mass M and dimensionless spin χ, we can define the characteristic length [98,99]

$$r_g = GM/c^2, \tag{1}$$

which is half the Schwarzchild radius r_s. The radius of the BH's outer horizon is [100]

$$r_+ = r_g \bar{r}_+ = r_g\left(1 + \sqrt{1-\chi^2}\right). \tag{2}$$

At the outer horizon, the frame-dragging angular velocity is [101]

$$\Omega_{\rm BH} = \frac{1}{2}\frac{c}{r_g}\frac{\chi}{\bar{r}_+}. \tag{3}$$

If there exist ULBs beyond the Standard Model particles, with mass [1–3]

$$m_b = \mu/c^2, \tag{4}$$

where μ is the rest energy, the angular frequency corresponding to the Compton wavelength $\lambda\!\!\!^{-}$ is [102]

$$\omega_\mu = c/\lambda\!\!\!^{-} = \mu/\hbar. \tag{5}$$

When a BH is born, the quantum fluctuations will lead to the pair production of particles in the vicinity of the BH. If the wavelength of the particles $\lambda\!\!\!^{-}$ is comparable to the Schwarzchild radius of the BH r_s, a process called

"superradiant instability" quickly extracts energy and angular momentum from the BH to increase the number of particles. Such a process occurs when the "superradiance condition" is satisfied [103],

$$\omega_\mu/m < \Omega_{\rm BH}, \tag{6}$$

where m is the magnetic quantum number, which is the projection of the particle's total angular momentum to the BH spin direction. As the field has nonzero mass, the bosons are gravitationally bound to the BH. The superradiance process continues to occur until Eq. (6) is no longer satisfied. The cloud can extract at most ∼10% of the BH's mass [104].

Interestingly, the structure of the cloud as well as the cloud solution is very similar to the electron cloud solution around a hydrogen atom (e.g., Refs. [16,24]). For this reason, it is convenient to define a so-called gravitational fine-structure constant α, which plays the same role as the fine-structure constant in the hydrogen atom and takes the value of the ratio of the two length scales [105,106]:

$$\alpha = \frac{r_g}{\lambda\!\!\!^{-}} = \frac{\frac{GM}{c^2}}{\frac{\hbar c}{\mu}} = \frac{G}{c^3\hbar} M\mu. \tag{7}$$

B. Gravitational-wave emission by the boson cloud

Once the boson cloud is of macroscopic size, it can emit gravitational radiation through three mechanisms [28]: (i) annihilation of bosons into gravitons; (ii) bosenova: the supernovalike collapse of the cloud due to boson self-interactions; and (iii) boson transitions between energy levels, analogous to electrons in the hydrogen atom. Bosenova signals (ii) last on the order of milliseconds [24,49,50], making bosenovae a better target for burstlike searches rather than continuous searches. The boson transitions between energy levels (iii) occur in very old BHs, but the remnants that we target are newborn black holes, which makes observations of these transitions unlikely in young merger remnants. Thus, here we focus on the first of the three mechanisms, annihilation of bosons into gravitons.

Hence, as in [28], in this work, we restrict ourselves to signals from annihilation only. We focus on the dominant level cloud, where the instability timescale is the shortest. For the dominant scalar cloud, $(n, l, j, m) = (2, 1, 1, 1)$, and for the dominant vector cloud, $(n, l, j, m) = (1, 0, 1, 1)$ where n, j, and m are the usual quantum numbers of the hydrogen atom. Including the higher-order modes may become important in a realistic search, but we expect that they would primarily introduce second-order corrections in our mock data analysis. The corrections could boost the signal strength and allow us to probe ultralight boson clouds slightly farther away and also enable one to perform a more rigorous parameter estimation for the ultralight bosons that could also test for jumps in the GW frequency caused by a jump in the cloud mode.

Here, we follow the approximations by [18,28,29,107], except for the gravitational-wave amplitude for the scalar boson, for which we adopt the nonrelativistic approximation. The boson cloud would emit quasimonochromatic GWs. The initial frequency of the CWs emitted by the boson cloud is

$$f_0 \approx 645\ {\rm Hz}\left(\frac{10M_\odot}{M}\right)\left(\frac{\alpha}{0.1}\right). \tag{8}$$

After formation, the frequency would increase over time since cloud mass decreases. The frequency drift is approximated by

$$\dot{f}^{(s)} \approx 3\times10^{-14}\ {\rm Hz/s}\left(\frac{10M_\odot}{M}\right)^2\left(\frac{\alpha}{0.1}\right)^{19}\chi^2 \tag{9}$$

for the dominant scalar mode and

$$\dot{f}^{(v)} \approx 1\times10^{-6}\ {\rm Hz/s}\left(\frac{10M_\odot}{M}\right)^2\left(\frac{\alpha}{0.1}\right)^{15}\chi^2 \tag{10}$$

for the dominant vector mode. The frequency drift is much faster for vector bosons than for scalar bosons because vector clouds emit gravitational waves at a faster rate.

When the BH has been fully spun down, the gravitational-wave strain amplitude emitted by the dominant mode boson cloud surrounding the BH is approximated by [28]

$$h^{(s)}_{0,\rm peak} \approx 2\times10^{-27}\left(\frac{M}{10M_\odot}\right)\left(\frac{\alpha}{0.1}\right)^7\left(\frac{\rm Mpc}{d_L}\right)\left(\frac{\chi-\chi_f}{0.1}\right) \tag{11}$$

for the dominant scalar mode and

$$h^{(v)}_{0,\rm peak} \approx 4\times10^{-24}\left(\frac{M}{10M_\odot}\right)\left(\frac{\alpha}{0.1}\right)^5\left(\frac{\rm Mpc}{d_L}\right)\left(\frac{\chi-\chi_f}{0.1}\right) \tag{12}$$

for the dominant vector mode. The strain of the annihilation is largest when the cloud first reaches the maximum occupation number. As the bosons annihilate and deplete the cloud, the strain amplitude $h_0(t)$ decreases over time,

$$h_0(t) \approx \frac{h_0}{1+\frac{t}{\tau_{GW}}}, \tag{13}$$

where τ_{GW} is the gravitational-wave timescale, which is the time it takes to radiate away half of the cloud's rest energy:

$$\begin{aligned}\tau^{(s)}_{GW} &\approx 6.5\times10^4\ {\rm yr}\left(\frac{M}{10M_\odot}\right)\left(\frac{0.1}{\alpha}\right)^{15}\frac{1}{\chi}.\\ \tau^{(v)}_{GW} &\approx 1\ {\rm day}\left(\frac{M}{10M_\odot}\right)\left(\frac{0.1}{\alpha}\right)^{11}\frac{1}{\chi}.\end{aligned} \tag{14}$$

Since the frequency evolution is slow, we approximate the gravitational waves emitted by the boson cloud to take the waveform $h(t)$ expanding the time evolution of the frequency in its first derivative only, such that

$$h(t) = h_{0,\mathrm{peak}}(t)e^{i\omega t} = \frac{h_{0,\mathrm{peak}}}{1+\frac{t}{\tau_{GW}}} e^{i2\pi(f_0+\dot{f}t)t}, \qquad (15)$$

where the angular frequency slowly evolves with time: $\omega = 2\pi(f_0 + \dot{f}t)$. Including higher-order derivatives or formulating a more complete waveform would allow for more accurate results. In particular, the nonrelativistic expression for the GW amplitude in the scalar and vector case is accurate within approximately an order of magnitude. Specifically, Refs. [32,95,108] find that the amplitude using full GR time-domain simulation may differ for the loudest signals by about an order of magnitude [109]. A similar correction may result in the gravitational-wave frequency drift. However, the principle test behind our analysis would be unchanged by such corrections.

C. Postmerger remnants

In the following sections, we will limit ourselves to clouds formed around binary BH merger remnants. It is advantageous to perform searches targeting postmerger remnants for the following reasons:

(1) By analyzing the GWs from the mergers, we know the location of the remnants. In addition to the three-detector network of LIGO Hanford, Livingston, and Virgo, KAGRA has become operational [110,111], and LIGO-India [112,113] is expected to become online in the coming years. Thus, in the future, we expect to be able to better localize merger events. Hence, after we detect signals from mergers, we can perform follow-up directed searches for ultralight boson clouds in the direction of the merger remnant [28].
(2) By analyzing the mergers waveform, we have information about BH mass M, BH spin χ, and luminosity distance d_L. From these, and combining the CW waveform, we can infer the boson mass μ.
(3) Four measurements are depending on μ: $f, \dot{f}, h_{0,\mathrm{peak}}$, τ_{GW}. By combining these four measurements with the parameters from the merger stated above, we can infer four independent μ, which can provide robust evidence for the existence of ULBs: if four measurements μ agree, it is very likely that ULBs exist, as there are no other reasons for all the μ to agree; if four measurements of μ differ, we can rule out the existence of ULBs at a particular mass range.
(4) Most importantly, we can rule out other possible CW sources, such as neutron stars, as it is unlikely that the signal is given by other CW sources if the measurements of boson properties agree.

Figure 1 shows an illustration of the setup we consider.

III. DETECTION HORIZON

A. Horizon calculation

Using the approximation in Sec. II B, we can find the detection horizon, where the signal is barely detectable, of ULB clouds formed around postmerger remnants by various GW observatories. As a rough approximation, we assume that a GW is detectable when its SNR is above 8. We note, however, that the typical continuous-wave searches utilize different search methodologies to the matched filtering (for example HMM), which may change the detectability slightly. However, because it may be challenging to use HMM to track vector modes that can evolve more rapidly than the scalar modes [28], we consider standard matched filtering here (although we note that it is in principle possible to tune the short Fourier transform length and coherent time in such a way as to accommodate the vector search). Therefore, the results here can be taken as an optimistic upper limit. A search with real data will likely benefit from the development of continuous-wave methodologies for the more rapidly evolving vector modes.

For the Fourier transformed amplitude $\tilde{h}(f)$, no analytical transformation exists, and it is computationally expensive to perform numerical transforms. As a result, we apply the stationary phase approximation here (see Appendix A for derivation):

$$\tilde{h}(f) \approx \frac{h_{0,\mathrm{peak}}}{1+\frac{f-f_0}{2\dot{f}\tau_{GW}}} \sqrt{\frac{i}{2\dot{f}}} \exp\left(-i2\pi\frac{(f-f_0)^2}{4\dot{f}}\right). \qquad (16)$$

Figure 2 shows the horizon at different masses by LIGO at design sensitivity [114], as well as next-generation ground-based GW observatories Cosmic Explorer [115–117].

We assume 3 years of observation time for scalar bosons and 1 day of observation time for vector bosons. We take $\chi = 0.7$, a value similar to the spin of most observed merger remnants [51,86,87]. We choose several values of α that would satisfy the "superradiance condition" specified in Eq. (6).

In Fig. 2, we also show the scatter of the merger population forecast obtained from [118]. As a summary of Ref. [118], the model uses the POWERLAW + PEAK mass model fitted to the O1 and O2 observations with a merger-rate density tracing the star-formation rate density as predicted by Pop-I/II stars and population synthesis codes (we refer the interested reader to the article itself for details). The observed rate of mergers ($\mathrm{SNR}_{\mathrm{merger}} > 8$) is $\sim$1900 yr^{-1}. Out of the $\sim$1900 mergers with $\mathrm{SNR}_{\mathrm{merger}} > 8$, four candidates clearly stand out in both scalar and vector cases. They are expected to host ULB clouds within the horizon of the LIGO detectors at design sensitivity ($\mathrm{SNR}_{\mathrm{cloud}} > 8$), meaning it may be possible to observe signals from such clouds soon. For scalar bosons,

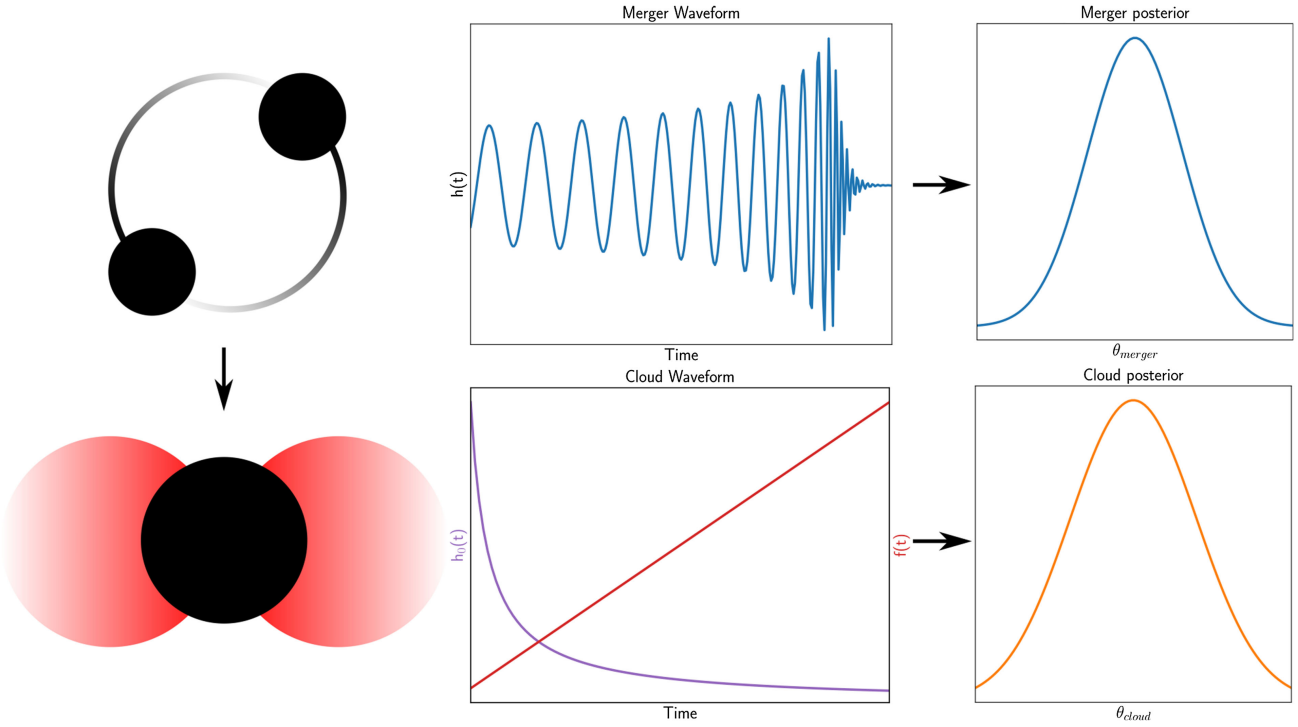

FIG. 1. An illustration of the search for ULBs using postmerger remnants. Top: when a system of binary black holes merges, it radiates gravitational waves, from which we can infer the parameters θ_{merger} of the binary black hole system. Bottom: due to superradiance, ultralight bosons form clouds around the rotating black hole merger remnant by extracting energy and angular momentum from it. As the mass of the boson cloud grows by spinning down the BH, the bosons simultaneously and with increasing efficiency annihilate to emit gravitational waves. We can infer the parameters θ_{cloud} of the black hole–boson cloud system by studying these gravitational waves. Combining both measurements, one could obtain robust evidence of the existence of ultralight bosons.

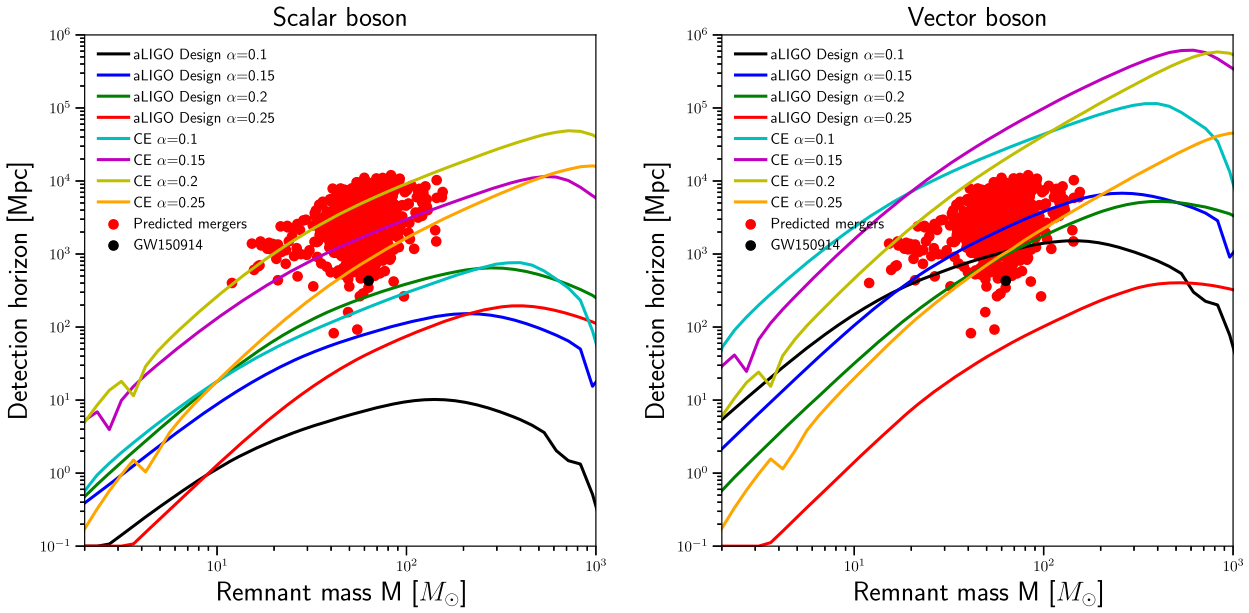

FIG. 2. Detection horizon of ULB cloud formed around merger remnants vs host BH mass by different detectors, along with the scatter of predicted and the observed binary BH merger event GW150914. The parameter space under the curve would be detectable by the respective detector. We take the initial spin being 0.7, a value similar to most known merger remnants. We choose several α values that would satisfy the superradiance condition specified in Eq. (6). We assume 3 years of observation time for scalar and 1 day of observation time for vector. For both scalar and vector, four golden merger remnants are predicted to host ULB clouds within the horizon of the LIGO detectors at design sensitivity.

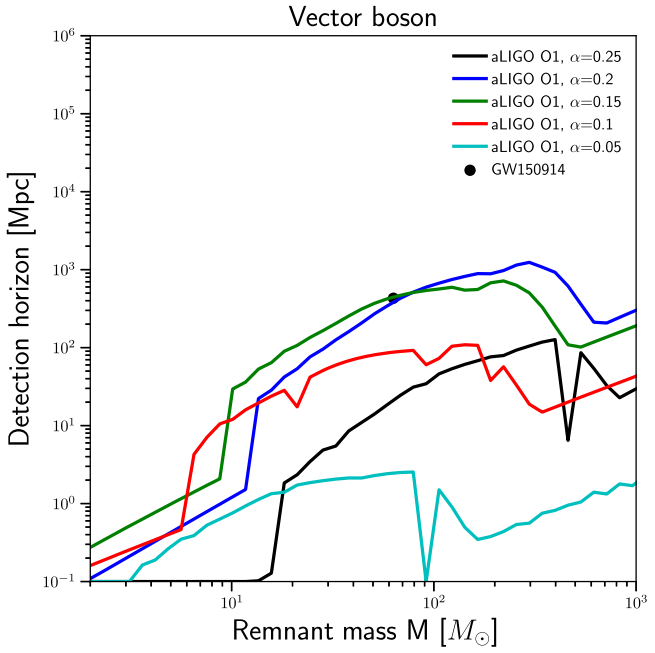

FIG. 3. Same horizon plot as in Fig. 2, but for the first run O1 [121] sensitivity. O1 sensitivity could be marginally detecting the vector boson cloud hosted by the remnant from the first gravitational-wave observation GW150914 [120], if the boson mass falls into the right range ($\alpha \sim 0.15$–0.2, which corresponds to a boson mass μ of 3.2×10^{-13}–4.3×10^{-13} eV).

GW150914 cannot host ULB clouds within the detection horizon at design sensitivity. However, we may turn our eyes toward the future to see the possibility of having such detection. Note, however, that these estimates are based on theoretical modeling of the merger-rate density, where there is some variation between different population synthesis models [119]. A more accurate estimate may become feasible in the future, as the number of gravitational-wave detections grows.

However, for vector boson, we might be able to detect a cloud hosted by the remnant of the observed merger; the first gravitation-wave observation event GW150914 was quite near and the spin, and mass of the remnant favor the formation of a detectable superradiant instability [120]. Indeed, it would be interesting to see if we would be able to detect the vector boson cloud hosted by the remnant of GW150914 in the observation run O1 data. Hence, we also obtain the vector horizon at O1 sensitivity in Fig. 3. If ULBs exist in the right mass range, with $\alpha \sim 0.15$–0.2, which corresponds to a boson mass μ of 3.2×10^{-13}–4.3×10^{-13}, our results suggest that O1 sensitivity may detect the boson cloud hosted by GW150914 or to partially rule out the relevant parameter space.

IV. ANALYSIS

To illustrate how one can combine the merger information with the binary information, we choose a binary merger event that formed detectable bosonic clouds around merger remnants from our catalog (Fig. 2). In particular, the parameters of the merger remnants are given in Table I. For these two remnants, we simulate the GW from both the merger signal (using the IMRPhenomPv2 waveform [122]) and the cloud signal [Eq. (16)]. We then independently infer the binary and the cloud parameters using the Bilby nested sampling tool and combine the measurements together.

TABLE I. Properties of one of the interesting remnants expected to host boson clouds within the detection horizon at LIGO at design sensitivity: mass of the binary BH before coalescence m_1 and m_2, mass of the remnant M, spin of the binary BH before coalescence χ_1 and χ_2, spin of the remnant χ, luminosity distance d_L, and SNR of the merger.

$m_1\,(M_\odot)$	$m_2\,(M_\odot)$	$M\,(M_\odot)$	χ_1	χ_2	χ	d_L (Mpc)	SNR
28.67	20.51	49.19	0.45	0.25	0.7	160.17	19.53

We find that by combining the merger signal and the cloud signal different inference schemes produce a single, consistent measurement of the boson cloud in the vector and scalar case (Fig. 4). Although we presume that the cloud waveform is precisely modeled, which is optimistic, the results demonstrate that the information from the boson cloud can be used to cross-verify the ultralight boson hypothesis in a way that is unique to merger remnants. For the scalar boson, the damping time τ_{GW} measurement cannot be well measured, as it is in the timescale of years, and thus the peak is a bit off compared with other measurements. In contrast, the τ_{GW} for the vector boson is in the timescale of days and can be well measured, thus showing a more consistent peak with other measurements.

We also perform the same analysis to see if we can disentangle the signal of scalar boson cloud from the vector boson cloud. To do this, we inject the GW signal by scalar boson cloud and infer the boson mass using the vector model. In Fig. 5, we show that if a scalar boson signal injection is analyzed with the vector model hypothesis we cannot obtain a consistent boson mass. Thus, our results suggest that we would be able to tell whether the signal comes from a scalar boson cloud or a vector boson cloud.

To see how the strategy helps us to distinguish signals from ULB cloud and other CW sources, we inject a CW signal from a pulsar and infer the signal using the boson cloud waveform. This ought to tell us whether or not it would be possible for other sources to mimic a ULB cloud signal. In Fig. 6, we show that if the signal is coming from a pulsar source, the inference would give inconsistent measurements of boson mass. In particular, we inject the signal from the Crab pulsar, with $f = 59.25$ Hz and $h_0 = 1.4 \times 10^{-24}$, assuming it radiates at the spindown

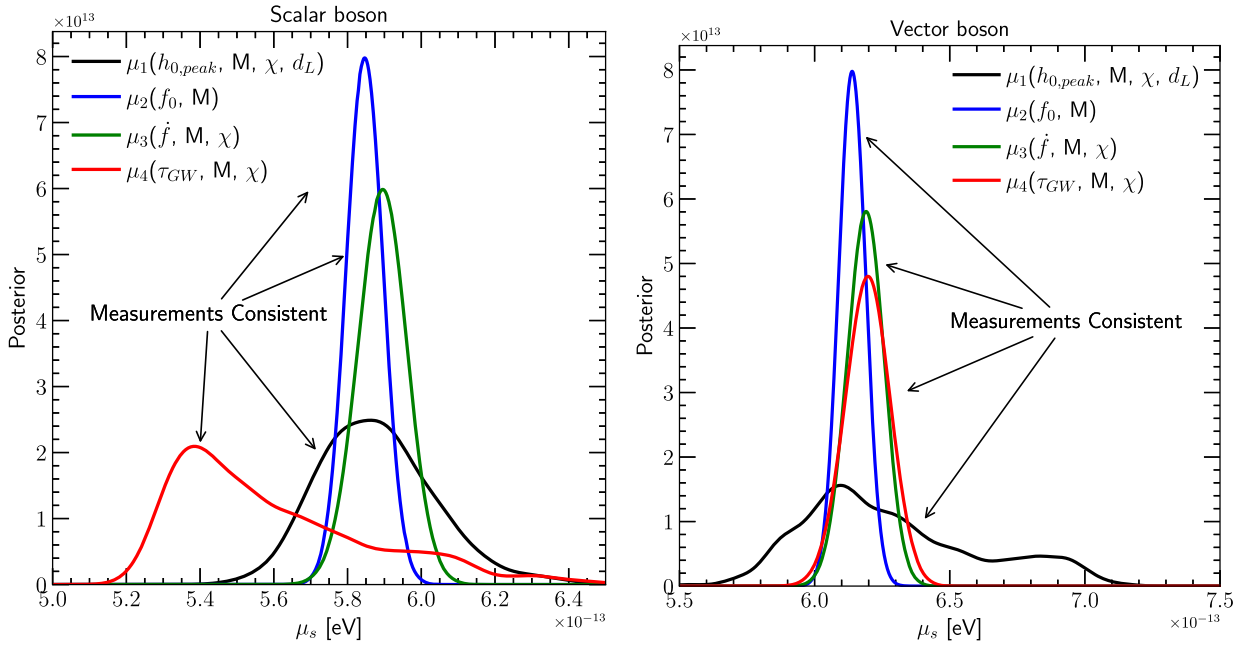

FIG. 4. An example of the posterior. If an ultralight boson exists in nature, the four different measurements of the gravitational waves emitted by the cloud would provide an agreed value of boson mass. Here, we use the binary black hole merger remnant system with properties listed in Table I and $\alpha = 0.2$ to simulate gravitation waves signal release by the merger and the ultralight boson cloud formed around the remnant. The SNR is 11.42 for the scalar cloud (left) and 46.06 for the vector cloud (right). We then perform parameter estimation using Bilby [123] to get the posterior from measurements of the merger and the cloud independently, which are then combined to obtain the posterior of boson mass. It shows the four posteriors of boson mass agree with each other, signifying the existence of an ultralight boson.

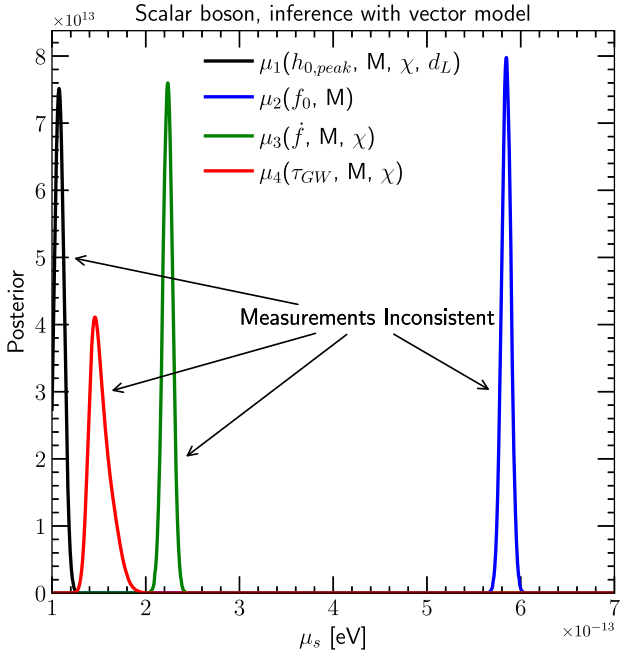

FIG. 5. Disentangling the signal between scalar and vector boson. To do so, we inject the GW signal from the scalar boson and infer the boson mass with vector model. The four measurements of the boson mass will not be consistent as in Fig. 4. Thus, we can distinguish whether the signal is from a scalar boson cloud or a vector boson cloud.

limit, and a very small value of $\dot{f}$ and a very large value of τ_{GW} [124] as an illustrative example. Therefore, by this analysis, we argue that it would be possible to distinguish ULB signals from other CW signals.[2]

To quantify the consistency of the measurements, we calculate the overlap Bayes factor following [125]

$$\mathcal{B} = \int \frac{P(\mu_1|d)P(\mu_2|d)P(\mu_3|d)P(\mu_4|d)}{P(\mu)^3} d\mu, \quad (17)$$

which measures how much the measurements overlap. If the measurements are consistent, they would have a larger overlapping region, which corresponds to a larger Bayes factor. The prior probability $P(\mu)$ is set to be uniform at 10^{-15}–10^{-10} eV, which corresponds to the frequency detectable by ground-based detectors [Eq. (8)]; we set $\mu_i = \mu$, by definition; and d stands for both data from the binary black hole merger and also the subsequent cloud waveform. Although the Bayes factor can be quite sensitive to the prior information, our results show that one can

[2]Though we also note that there may be other ways to discriminate between the different sources, for example, GWs from spinning neutron stars typically decrease in frequency while GWs from boson clouds typically increase in frequency.

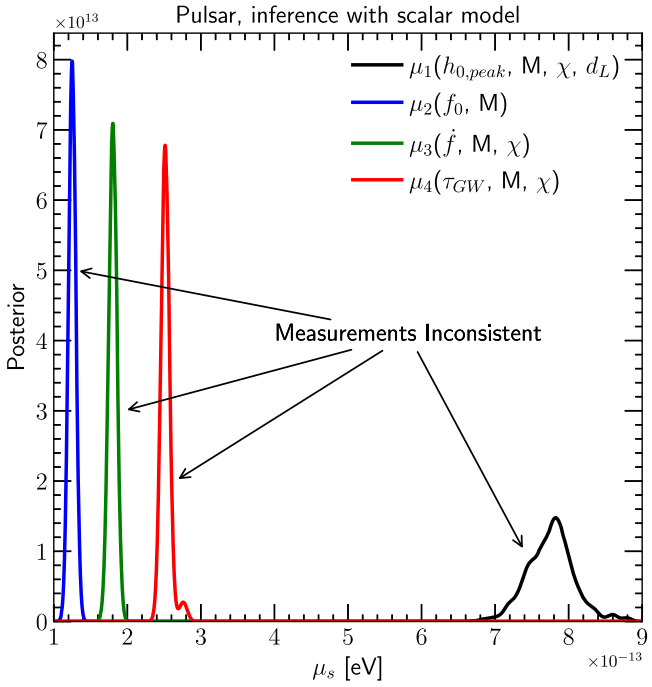

FIG. 6. The analysis can be used to distinguish CW signals from ULB cloud and other sources. We inject GW signal from a pulsar and infer the boson mass. Four measurements of the boson mass are not consistent; hence, we can distinguish whether the signal is from the ULB cloud or other sources.

robustly quantify the overlap and lack thereof. Indeed, in Table II, we summarize the Bayes factor for each of the measurements. The Bayes factors for the scalar injection scalar hypothesis and vector injection vector hypothesis are large positive numbers due to the heavy overlap in posteriors. On the other hand, for the case of scalar signal injection with vector hypothesis, and pulsar signal injection, the Bayes factor is zero due to the inconsistent measurements of boson mass.

TABLE II. Overlap Bayes factor of each signal analyzed. We show the injected signal (left column), the hypothesis that we consider in estimating the Bayes factor (middle column), and the overlap Bayes factor (right column). The Bayes factor [Eq. (17)] quantifies how much each measurement overlaps with each other. The more consistent the measurements are, the higher the Bayes factor. The Bayes factor correctly identifies the scalar/vector cloud when one is injected into the data and can also rule out the incorrect hypothesis when attempting to infer the parameters of a simulated waveform using a different hypothesis.

Injection	Hypothesis	Overlap Bayes factor
Scalar	Scalar	7.3×10^9
Vector	Vector	2.5×10^{11}
Scalar	Vector	0
Pulsar	Scalar	0

V. CONCLUSIONS AND OUTLOOK

We have quantified the horizon for finding boson clouds around merger remnants. By comparing with the existing forecast on merger events, we find that we may detect signals from boson clouds formed around merger remnants in the near future. In estimating the horizon distance, since no analytical transform is available, we use stationary phase approximation to perform the Fourier transform of the wave. To perform actual searches, dedicated continuous wave approaches and more sophisticated approaches would be needed. Furthermore, the estimates need to be interpreted with some care as they are to a degree subject to the changes in the merger-rate density, which suffer from uncertainty at high redshift (e.g., Ref. [119]; see also the discussion in Ref. [118]). Nevertheless, the current results outline a possible scenario. Interestingly, we also find that if ULBs are vector bosons and in the right mass range the ground-based detectors may already have detected the signal of the boson cloud hosted by GW150914.

Targeting merger remnants can indeed be a good strategy as it could provide a consistency test that might cross-verify the existence of ULBs. In particular, when the signal is produced by other CW sources, the measurement of boson mass will be inconsistent, which can help us to confirm if the source of the CW is the ULB cloud. Thus, the test would be able to disentangle between other continuous-wave sources and genuine ultralight boson signals at great accuracy. Furthermore, the same method would be able to disentangle between vector bosons and scalar bosons with great accuracy. This may provide a complementary strategy to other detection methods when we receive CW signals. Indeed, although targeting merger remnants may have the disadvantage of having a lower rate of detections compared to some of the alternatives [28], it has the advantage of being able to robustly confirm that the signal indeed originates from an ultralight boson cloud. Since a robust verification of any new particle would likely require extraordinary evidence, a corroborating detection from a merger remnant in the scenario that ultralight bosons do exist would be quite valuable.

In the future, the proof-of-concept analysis we have presented here will hopefully find applications to real data. To this end, future work may focus on building more sophisticated analyses targeting continuous waves with a rapid frequency drift, such as those expected from vector bosons. To this end, it will become more important to also include higher-order corrections to the gravitational-wave waveform and more agnostic search strategies; work toward a practical search strategy is being carried out by Ref. [126]. Another important aspect in future analyses will also be to account for Earth's rotation, as the signals we target can last up to years. Nevertheless, the proof-of-concept analysis presented here demonstrates the potential for an interesting consistency test with merger remnants.

ACKNOWLEDGMENTS

We thank Richard Brito, Isaac C. F. Wong, William East, and Ling Sun for their useful comments and suggestions. O. A. H. is partially supported by grants from the Research Grants Council of Hong Kong, The Croucher Foundation of Hong Kong, and the Research Committee of the Chinese University of Hong Kong. We acknowledge the software packages used, including Matplotlib [127], NumPy [128], SciPy [129], SCIKIT-LEARN [130], Bilby [123], and PyCBC [131]. The authors are grateful for computational resources provided by the LIGO Laboratory and supported by National Science Foundation Grants No. PHY-0757058 and No. PHY-0823459. This material is based upon work supported by NSF's LIGO Laboratory, which is a major facility fully funded by the National Science Foundation. K. H. M. C. and O. A. H. acknowledge support by grants from the Research Grants Council of Hong Kong (Projects No. CUHK 14304622 and No. 14307923), the start-up grant from the Chinese University of Hong Kong, and the Direct Grant for Research from the Research Committee of The Chinese University of Hong Kong.

APPENDIX A: STATIONARY PHASE APPROXIMATION, LIKELIHOOD, AND SIGNAL-TO-NOISE RATIO

In this appendix, we provide the calculation of $\tilde{h}(f)$ using the stationary phase approximation. The Fourier transform of the time-domain strain $h(t)$ is given by

$$\tilde{h}(f) = \int h(t) e^{-i2\pi f t} dt \tag{A1}$$

$$= \int \frac{h_{0,\mathrm{peak}}}{1+\frac{t}{\tau_{GW}}} \exp(i2\pi(f_0 + \dot{f}t - f)t) dt \tag{A2}$$

$$= \int \frac{h_{0,\mathrm{peak}}}{1+\frac{t}{\tau_{GW}}} \exp(i2\pi\Phi(t)) dt, \tag{A3}$$

where phase $\Phi(t) = f_0 t + \dot{f}t^2 + ft$. The first derivative of phase $\Phi(t)$ is

$$\Phi'(t) = f_0 + 2\dot{f}t - f, \tag{A4}$$

and the second derivative is

$$\Phi''(t) = 2\dot{f}. \tag{A5}$$

For stationary phase approximation, the phase term is stationary when $\Phi'(t)|_{t=t_0} = 0$. By (A4), it is equivalent to

$$t_0 = \frac{f - f_0}{2\dot{f}}. \tag{A6}$$

Putting t_0 back into $\Phi(t)$ and $h_0(t)$,

$$\Phi(t_0) = -\frac{(f-f_0)^2}{4\dot{f}}, \tag{A7}$$

and

$$h_0(t_0) = \frac{h_{0,\mathrm{peak}}}{1+\frac{f-f_0}{2\dot{f}\tau_{GW}}}. \tag{A8}$$

If we expand $\Phi(t)$ as a Taylor series about t_0 to the second order,

$$\Phi(t) \approx \Phi(t_0) + \frac{1}{2}\Phi''(t_0)(t-t_0)^2 \tag{A9}$$

$$= -\frac{(f-f_0)^2}{4\dot{f}} + \dot{f}(t-t_0)^2. \tag{A10}$$

Putting the results of (A8) and (A10) back into (A1),

$$\tilde{h}(f) = \int h_0(t_0) \exp\left[i2\pi(\Phi(t_0) + \frac{\Phi''}{2}(t_0)(t-t_0)^2)\right] dt \tag{A11}$$

$$= h_0(t_0)\exp(i2\pi\Phi(t_0)) \int \exp(i2\pi\dot{f}(t-t_0)^2) dt \tag{A12}$$

$$= \frac{h_{0,\mathrm{peak}}}{1+\frac{f-f_0}{2\dot{f}\tau_{GW}}} \sqrt{\frac{i}{2\dot{f}}} \exp\left(-i2\pi\frac{(f-f_0)^2}{4\dot{f}}\right), \tag{A13}$$

where in the final line we have used the result $\int \exp(\frac{1}{2}icx^2)dx = \sqrt{2i\pi/c}$.

Our likelihood then follows the standard likelihood (e.g., Ref. [124])

$$\mathcal{L}(\theta) = (d - h(\theta), d - h(\theta)), \tag{A14}$$

where the inner product

$$(a,b) = 4\int_0^\infty \frac{a(f)b^*(f)}{S_n(f)} df, \tag{A15}$$

where $S_n(f)$ is the power spectral density of the noise of a detector that we obtain from LALSuite [122]. Since the inner product is difficult to integrate numerically due to the lengthy duration of the data, we solve it by plugging in the analytical solution of the waveform [Eq. (A11)] and assuming that the data consists of the waveform only ($d = h_{\mathrm{true}} + n \approx h_{\mathrm{true}}$). The approach neglects some of the biases induced by the noise realization, similar to the Fisher Information Matrix approach [132], but does not assume a multivariate Gaussian form for the posterior distribution. Thus, in the high signal-to-noise ratio limit, we expect it to be reasonably accurate as long as the waveform is sufficiently well known, for proof-of-principle applications. We perform all parameter estimation with the Bilby software package [123]. For the binary inspiral, we use the standard approach implemented in the same software and perform the sampling in the full 15-dimensional space (for the likelihood definition and details, refer to Ref. [123]).

Using $\tilde{h}(f)$ in the form given in Eq. (A13), we calculate the horizon when the SNR is > 8. The SNR ρ is given by

$$\rho = \sqrt{(h,h)}. \tag{A16}$$

APPENDIX B: ULTRALIGHT BOSON MASS INFERENCE

Since our consistency test is made using independent measurements of the ultralight boson masses, here we briefly recap the precise form of the independent boson mass measurements. In particular, using the GW emission equations given in Sec. II B, the boson masses

$$\begin{aligned}
\mu_1^{(s)} &= \mu_1(h_{0,\mathrm{peak}}^{(s)}, M, \chi, d_L) \\
&= \frac{0.1c^3\hbar}{GM}\sqrt[7]{\frac{h_{0,\mathrm{peak}}^{(s)}}{8\times10^{-28}}\frac{10M_\odot}{M}\frac{d_L}{\mathrm{Mpc}}\frac{0.1}{\chi-\chi_f}} \\
\mu_2^{(s)} &= \mu_2(f_0, M) \\
&= \frac{0.1c^3\hbar}{GM}\frac{f_0}{645Hz}\frac{10M_\odot}{M} \\
\mu_3^{(s)} &= \mu_3(\dot{f}^{(s)}, M) \\
&= \frac{0.1c^3\hbar}{GM}\sqrt[19]{\frac{\dot{f}^{(s)}}{3\times10^{-14}Hz/s}\left(\frac{M}{10M_\odot}\right)^2\frac{1}{\chi^2}} \\
\mu_4^{(s)} &= \mu_4(\tau_{GW}^{(s)}, M, \chi) \\
&= \frac{0.1c^3\hbar}{GM}\sqrt[15]{\frac{6.5\times10^4 yr}{\tau_{GW}^{(s)}}\frac{M}{10M_\odot}\frac{1}{\chi}}
\end{aligned} \tag{B1}$$

for the scalar boson case and

$$\begin{aligned}
\mu_1^{(v)} &= \mu_1(h_{0,\mathrm{peak}}^{(v)}, M, \chi, d_L) \\
&= \frac{0.1c^3\hbar}{GM}\sqrt[5]{\frac{h_{0,\mathrm{peak}}^{(v)}}{4\times10^{-24}}\frac{10M_\odot}{M}\frac{d_L}{\mathrm{Mpc}}\frac{0.1}{\chi-\chi_f}} \\
\mu_2^{(v)} &= \mu_2(f_0, M) \\
&= \frac{0.1c^3\hbar}{GM}\frac{f_0}{645Hz}\frac{10M_\odot}{M} \\
\mu_3^{(v)} &= \mu_3(\dot{f}^{(v)}, M) \\
&= \frac{0.1c^3\hbar}{GM}\sqrt[15]{\frac{\dot{f}^{(s)}}{1\times10^{-6}Hz/s}\left(\frac{M}{10M_\odot}\right)^2\frac{1}{\chi^2}} \\
\mu_4^{(v)} &= \mu_4(\tau_{GW}^{(v)}, M, \chi) \\
&= \frac{0.1c^3\hbar}{GM}\sqrt[11]{\frac{1\mathrm{day}}{\tau_{GW}^{(v)}}\frac{M}{10M_\odot}\frac{1}{\chi}}
\end{aligned} \tag{B2}$$

for vector boson. The four inferred boson mass μ can then be used to cross-verify the existence of ultralight bosons. Most notably, without the measurement of the mass and spin from the binary inspiral, it is not generally possible to retrieve the four independent measurements of the ultralight boson masses. That is, observing the binary black hole merger is the key in being able to perform the consistency test advocated for here.

[1] R. D. Peccei and H. R. Quinn, Constraints imposed by CP conservation in the presence of pseudoparticles, Phys. Rev. D **16**, 1791 (1977).
[2] S. Weinberg, A new light boson?, Phys. Rev. Lett. **40**, 223 (1978).
[3] F. Wilczek, Problem of strong P and T invariance in the presence of instantons, Phys. Rev. Lett. **40**, 279 (1978).
[4] J. Preskill, M. B. Wise, and F. Wilczek, Cosmology of the invisible axion, Phys. Lett. **120B**, 127 (1983).
[5] M. I. Khlopov, B. A. Malomed, and I. B. Zeldovich, Gravitational instability of scalar fields and formation of primordial black holes, Mon. Not. R. Astron. Soc. **215**, 575 (1985).
[6] A. Arvanitaki, J. Huang, and K. Van Tilburg, Searching for dilaton dark matter with atomic clocks, Phys. Rev. D **91**, 015015 (2015).
[7] Y. Chikashige, R. Mohapatra, and R. Peccei, Are there real Goldstone bosons associated with broken lepton number?, Phys. Lett. **98B**, 265 (1981).
[8] G. Bertone, D. Hooper, and J. Silk, Particle dark matter: Evidence, candidates and constraints, Phys. Rep. **405**, 279 (2005).
[9] L. Ackerman, M. R. Buckley, S. M. Carroll, and M. Kamionkowski, Dark matter and dark radiation, Phys. Rev. D **79**, 023519 (2009).
[10] M. Fairbairn, R. Hogan, and D. J. E. Marsh, Unifying inflation and dark matter with the Peccei-Quinn field: Observable axions and observable tensors, Phys. Rev. D **91**, 023509 (2015).
[11] D. J. E. Marsh, D. Grin, R. Hlozek, and P. G. Ferreira, Tensor detection severely constrains axion dark matter, Phys. Rev. Lett. **113**, 011801 (2014).

[12] D. J. E. Marsh, Axion cosmology, Phys. Rep. **643**, 1 (2016).
[13] G. Bertone and D. Hooper, History of dark matter, Rev. Mod. Phys. **90**, 045002 (2018).
[14] E. Braaten and H. Zhang, Colloquium: The physics of axion stars, Rev. Mod. Phys. **91**, 041002 (2019).
[15] M. P. Hertzberg, M. Tegmark, and F. Wilczek, Axion cosmology and the energy scale of inflation, Phys. Rev. D **78**, 083507 (2008).
[16] A. Arvanitaki, S. Dimopoulos, S. Dubovsky, N. Kaloper, and J. March-Russell, String axiverse, Phys. Rev. D **81**, 123530 (2010).
[17] S. Asztalos *et al.* (ADMX Collaboration), A SQUID-based microwave cavity search for dark-matter axions, Phys. Rev. Lett. **104**, 041301 (2010).
[18] A. Arvanitaki and S. Dubovsky, Exploring the string axiverse with precision black hole physics, Phys. Rev. D **83**, 044026 (2011).
[19] J. E. Kim and D. J. E. Marsh, An ultralight pseudoscalar boson, Phys. Rev. D **93**, 025027 (2016).
[20] L. Hui, J. P. Ostriker, S. Tremaine, and E. Witten, Ultralight scalars as cosmological dark matter, Phys. Rev. D **95**, 043541 (2017).
[21] A. Arvanitaki, S. Dimopoulos, M. Galanis, L. Lehner, J. O. Thompson, and K. Van Tilburg, Large-misalignment mechanism for the formation of compact axion structures: Signatures from the QCD axion to fuzzy dark matter, Phys. Rev. D **101**, 083014 (2020).
[22] V. M. Mehta, M. Demirtas, C. Long, D. J. E. Marsh, L. McAllister, and M. J. Stott, Superradiance exclusions in the landscape of Type IIB string theory, arXiv:2011.08693.
[23] L. Hui, Wave dark matter, Annu. Rev. Astron. Astrophys. **59**, 247 (2021).
[24] R. Brito, V. Cardoso, and P. Pani, Superradiance: New frontiers in black hole physics, Lect. Notes Phys. **906**, 1 (2015).
[25] T. Damour, N. Deruelle, and R. Ruffini, On quantum resonances in stationary geometries, Lett. Nuovo Cimento (1971–1985) **15**, 257 (1976).
[26] T. J. Zouros and D. M. Eardley, Instabilities of massive scalar perturbations of a rotating black hole, Ann. Phys. (N.Y.) **118**, 139 (1979).
[27] D. Baumann, H. S. Chia, J. Stout, and L. ter Haar, The spectra of gravitational atoms, J. Cosmol. Astropart. Phys. 12 (2019) 006.
[28] M. Isi, L. Sun, R. Brito, and A. Melatos, Directed searches for gravitational waves from ultralight bosons, Phys. Rev. D **99**, 084042 (2019).
[29] M. Baryakhtar, R. Lasenby, and M. Teo, Black hole superradiance signatures of ultralight vectors, Phys. Rev. D **96**, 035019 (2017).
[30] R. Brito, S. Grillo, and P. Pani, Black hole superradiant instability from ultralight spin-2 fields, Phys. Rev. Lett. **124**, 211101 (2020).
[31] A. Arvanitaki, M. Baryakhtar, and X. Huang, Discovering the QCD axion with black holes and gravitational waves, Phys. Rev. D **91**, 084011 (2015).
[32] R. Brito, S. Ghosh, E. Barausse, E. Berti, V. Cardoso, I. Dvorkin, A. Klein, and P. Pani, Gravitational wave searches for ultralight bosons with LIGO and LISA, Phys. Rev. D **96**, 064050 (2017).
[33] L. Tsukada, T. Callister, A. Matas, and P. Meyers, First search for a stochastic gravitational-wave background from ultralight bosons, Phys. Rev. D **99**, 103015 (2019).
[34] R. Brito, S. Ghosh, E. Barausse, E. Berti, V. Cardoso, I. Dvorkin, A. Klein, and P. Pani, Stochastic and resolvable gravitational waves from ultralight bosons, Phys. Rev. Lett. **119**, 131101 (2017).
[35] X.-L. Fan and Y.-B. Chen, Stochastic gravitational-wave background from spin loss of black holes, Phys. Rev. D **98**, 044020 (2018).
[36] R. Roy, S. Vagnozzi, and L. Visinelli, Superradiance evolution of black hole shadows revisited, Phys. Rev. D **105**, 083002 (2022).
[37] Y. Chen, R. Roy, S. Vagnozzi, and L. Visinelli, Superradiant evolution of the shadow and photon ring of Sgr $A^\star$, Phys. Rev. D **106**, 043021 (2022).
[38] M. C. Ferreira, C. F. B. Macedo, and V. Cardoso, Orbital fingerprints of ultralight scalar fields around black holes, Phys. Rev. D **96**, 083017 (2017).
[39] D. Baumann, H. S. Chia, and R. A. Porto, Probing ultralight bosons with binary black holes, Phys. Rev. D **99**, 044001 (2019).
[40] O. A. Hannuksela, K. W. K. Wong, R. Brito, E. Berti, and T. G. F. Li, Probing the existence of ultralight bosons with a single gravitational-wave measurement, Nat. Astron. **3**, 447 (2019).
[41] D. Baumann, H. S. Chia, R. A. Porto, and J. Stout, Gravitational collider physics, Phys. Rev. D **101**, 083019 (2020).
[42] J. Zhang and H. Yang, Gravitational floating orbits around hairy black holes, Phys. Rev. D **99**, 064018 (2019).
[43] N. Bar, K. Blum, T. Lacroix, and P. Panci, Looking for ultralight dark matter near supermassive black holes, J. Cosmol. Astropart. Phys. 07 (2019) 045.
[44] E. Berti, R. Brito, C. F. B. Macedo, G. Raposo, and J. L. Rosa, Ultralight boson cloud depletion in binary systems, Phys. Rev. D **99**, 104039 (2019).
[45] A. Amorim *et al.* (GRAVITY Collaboration), Scalar field effects on the orbit of S2 star, Mon. Not. R. Astron. Soc. **489**, 4606 (2019).
[46] V. Cardoso, F. Duque, and T. Ikeda, Tidal effects and disruption in superradiant clouds: A numerical investigation, Phys. Rev. D **101**, 064054 (2020).
[47] M. Boskovic, R. Brito, V. Cardoso, T. Ikeda, and H. Witek, Axionic instabilities and new black hole solutions, Phys. Rev. D **99**, 035006 (2019).
[48] F. V. Day and J. I. McDonald, Axion superradiance in rotating neutron stars, J. Cosmol. Astropart. Phys. 10 (2019) 051.
[49] W. E. East, Vortex string formation in black hole superradiance of a dark photon with the Higgs mechanism, Phys. Rev. Lett. **129**, 141103 (2022).
[50] M. Baryakhtar, M. Galanis, R. Lasenby, and O. Simon, Black hole superradiance of self-interacting scalar fields, Phys. Rev. D **103**, 095019 (2021).
[51] R. Abbott *et al.* (The LIGO Scientific, Virgo, and KAGRA Collaborations), GWTC-3: Compact binary coalescences

observed by LIGO and Virgo during the second part of the third observing run, Phys. Rev. X **13**, 041039 (2023).
[52] G. Bertone, D. Croon, M. Amin, K. K. Boddy, B. Kavanagh, K. J. Mack *et al.*, Gravitational wave probes of dark matter: Challenges and opportunities, SciPost Phys. Core **3**, 007 (2020).
[53] R. Abbott, H. Abe, F. Acernese, K. Ackley, N. Adhikari, R. Adhikari *et al.*, All-sky search for gravitational wave emission from scalar boson clouds around spinning black holes in LIGO O3 data, Phys. Rev. D **105**, 102001 (2022).
[54] R. Abbott, T. D. Abbott, F. Acernese *et al.* (The LIGO Scientific, Virgo, and KAGRA Collaborations), Search for subsolar-mass binaries in the first half of Advanced LIGO and Virgo's third observing run, Phys. Rev. Lett. **129**, 061104 (2022).
[55] R. Abbott *et al.* (LIGO Scientific, Virgo, and KAGRA Collaborations), Constraints on dark photon dark matter using data from LIGO's and Virgo's third observing run, Phys. Rev. D **105**, 063030 (2022).
[56] A. Wagner *et al.* (ADMX Collaboration), A search for hidden sector photons with ADMX, Phys. Rev. Lett. **105**, 171801 (2010).
[57] G. Rybka *et al.* (ADMX Collaboration), A search for scalar chameleons with ADMX, Phys. Rev. Lett. **105**, 051801 (2010).
[58] S. Aune *et al.* (CAST Collaboration), CAST search for sub-eV mass solar axions with ^{3}He buffer gas, Phys. Rev. Lett. **107**, 261302 (2011).
[59] P. Pugnat *et al.* (OSQAR Collaboration), Search for weakly interacting sub-eV particles with the OSQAR laser-based experiment: Results and perspectives, Eur. Phys. J. C **74**, 3027 (2014).
[60] A. Arvanitaki, J. Huang, and K. Van Tilburg, Searching for dilaton dark matter with atomic clocks, Phys. Rev. D **91**, 015015 (2015).
[61] P. Corasaniti, S. Agarwal, D. Marsh, and S. Das, Constraints on dark matter scenarios from measurements of the galaxy luminosity function at high redshifts, Phys. Rev. D **95**, 083512 (2017).
[62] J. Choi, H. Themann, M. Lee, B. Ko, and Y. Semertzidis, First axion dark matter search with toroidal geometry, Phys. Rev. D **96**, 061102 (2017).
[63] D. Akerib *et al.* (LUX Collaboration), First searches for axions and axionlike particles with the LUX experiment, Phys. Rev. Lett. **118**, 261301 (2017).
[64] B. Brubaker *et al.*, First results from a microwave cavity axion search at 24 μeV, Phys. Rev. Lett. **118**, 061302 (2017).
[65] Y. J. Kim, P.-H. Chu, and I. Savukov, Experimental constraint on an exotic spin- and velocity-dependent interaction in the sub-meV range of axion mass with a spin-exchange relaxation-free magnetometer, Phys. Rev. Lett. **121**, 091802 (2018).
[66] A. Garcon *et al.*, The cosmic axion spin precession experiment (CASPEr): A dark-matter search with nuclear magnetic resonance, Quantum Sci. Technol. **3**, 014008 (2017).
[67] A. Arvanitaki, M. Baryakhtar, S. Dimopoulos, S. Dubovsky, and R. Lasenby, Black hole mergers and the QCD axion at Advanced LIGO, Phys. Rev. D **95**, 043001 (2017).
[68] V. Cardoso, O. J. C. Dias, G. S. Hartnett, M. Middleton, P. Pani, and J. E. Santos, Constraining the mass of dark photons and axion-like particles through black-hole superradiance, J. Cosmol. Astropart. Phys. 03 (2018) 043.
[69] S. D'Antonio *et al.*, Semicoherent analysis method to search for continuous gravitational waves emitted by ultralight boson clouds around spinning black holes, Phys. Rev. D **98**, 103017 (2018).
[70] S. Ghosh, E. Berti, R. Brito, and M. Richartz, Follow-up signals from superradiant instabilities of black hole merger remnants, Phys. Rev. D **99**, 104030 (2019).
[71] M. J. Stott, D. J. E. Marsh, C. Pongkitivanichkul, L. C. Price, and B. S. Acharya, Spectrum of the axion dark sector, Phys. Rev. D **96**, 083510 (2017).
[72] J. L. Ouellet *et al.*, First results from ABRACADABRA-10 cm: A search for Sub-μeV axion dark matter, Phys. Rev. Lett. **122**, 121802 (2019).
[73] H. Davoudiasl and P. B. Denton, Ultralight boson dark matter and event horizon telescope observations of M87*, Phys. Rev. Lett. **123**, 021102 (2019).
[74] N. Fernandez, A. Ghalsasi, and S. Profumo, Superradiance and the spins of black holes from LIGO and x-ray binaries, arXiv:1911.07862.
[75] C. Palomba *et al.*, Direct constraints on ultra-light boson mass from searches for continuous gravitational waves, Phys. Rev. Lett. **123**, 171101 (2019).
[76] K. K. Ng, M. Isi, C.-J. Haster, and S. Vitale, Multiband gravitational-wave searches for ultralight bosons, Phys. Rev. D **102**, 083020 (2020).
[77] C. Abel *et al.*, Search for axionlike dark matter through nuclear spin precession in electric and magnetic fields, Phys. Rev. X **7**, 041034 (2017).
[78] H. Grote and Y. V. Stadnik, Novel signatures of dark matter in laser-interferometric gravitational-wave detectors, Phys. Rev. Res. **1**, 033187 (2019).
[79] P. S. B. Dev, M. Lindner, and S. Ohmer, Gravitational waves as a new probe of Bose–Einstein condensate dark matter, Phys. Lett. B **773**, 219 (2017).
[80] S. J. Zhu, M. Baryakhtar, M. A. Papa, D. Tsuna, N. Kawanaka, and H.-B. Eggenstein, Characterizing the continuous gravitational-wave signal from boson clouds around Galactic isolated black holes, Phys. Rev. D **102**, 063020 (2020).
[81] K. K. Y. Ng, S. Vitale, O. A. Hannuksela, and T. G. F. Li, Constraints on ultralight scalar bosons within black hole spin measurements from the LIGO-Virgo GWTC-2, Phys. Rev. Lett. **126**, 151102 (2021).
[82] R. A. Remillard and J. E. McClintock, X-ray properties of black-hole binaries, Annu. Rev. Astron. Astrophys. **44**, 49 (2006).
[83] M. Middleton, *Black Hole Spin: Theory and Observation*, Astrophysics and Space Science Library Vol. 440 (2016), p. 99, 10.1007/978-3-662-52859-4_3.
[84] J. M. Corral-Santana, J. Casares, T. Munoz-Darias, F. E. Bauer, I. G. Martinez-Pais, and D. M. Russell, BlackCAT: A catalogue of stellar-mass black holes in x-ray transients, Astron. Astrophys. **587**, A61 (2016).

[85] K. K. Y. Ng, O. A. Hannuksela, S. Vitale, and T. G. F. Li, Searching for ultralight bosons within spin measurements of a population of binary black hole mergers, Phys. Rev. D **103**, 063010 (2021).
[86] B. Abbott, R. Abbott, T. Abbott, S. Abraham, F. Acernese, K. Ackley *et al.*, GWTC-1: A gravitational-wave transient catalog of compact binary mergers observed by LIGO and Virgo during the first and second observing runs, Phys. Rev. X **9**, 031040 (2019).
[87] R. Abbott, T. Abbott, S. Abraham, F. Acernese, K. Ackley, A. Adams *et al.*, GWTC-2: Compact binary coalescences observed by LIGO and Virgo during the first half of the third observing run, Phys. Rev. X **11**, 021053 (2021).
[88] Q. Yang, L.-W. Ji, B. Hu, Z.-J. Cao, and R.-G. Cai, An axion-like scalar field environment effect on binary black hole merger, Res. Astron. Astrophys. **18**, 065 (2018).
[89] L. Annulli, V. Cardoso, and R. Vicente, Response of ultralight dark matter to supermassive black holes and binaries, Phys. Rev. D **102**, 063022 (2020).
[90] B. J. Kavanagh, D. A. Nichols, G. Bertone, and D. Gaggero, Detecting dark matter around black holes with gravitational waves: Effects of dark-matter dynamics on the gravitational waveform, Phys. Rev. D **102**, 083006 (2020).
[91] A. K.-W. Chung, J. Gais, M. H.-Y. Cheung, and T. G. F. Li, Searching for ultralight bosons with supermassive black hole ringdown, Phys. Rev. D **104**, 084028 (2021).
[92] K. Riles, Recent searches for continuous gravitational waves, Mod. Phys. Lett. A **32**, 1730035 (2017).
[93] P. Pani, V. Cardoso, L. Gualtieri, E. Berti, and A. Ishibashi, Perturbations of slowly rotating black holes: Massive vector fields in the Kerr metric, Phys. Rev. D **86**, 104017 (2012).
[94] J. G. Rosa and S. R. Dolan, Massive vector fields on the Schwarzschild spacetime: Quasinormal modes and bound states, Phys. Rev. D **85**, 044043 (2012).
[95] W. E. East, Superradiant instability of massive vector fields around spinning black holes in the relativistic regime, Phys. Rev. D **96**, 024004 (2017).
[96] R. Brito, V. Cardoso, and P. Pani, Massive spin-2 fields on black hole spacetimes: Instability of the Schwarzschild and Kerr solutions and bounds on the graviton mass, Phys. Rev. D **88**, 023514 (2013).
[97] R. P. Kerr, Gravitational field of a spinning mass as an example of algebraically special metrics, Phys. Rev. Lett. **11**, 237 (1963).
[98] K. Schwarzschild, Über das Gravitationsfeld eines Massenpunktes nach der Einsteinschen Theorie, Sitzungsber. K. Preuss. Akad. Wiss. 189 (1916), https://ui.adsabs.harvard.edu/abs/1916SPAW.....189S.
[99] K. Schwarzschild, Über das Gravitationsfeld einer Kugel aus inkompressibler Flüssigkeit nach der Einsteinschen Theorie, Sitzungsber. K. Preuss. Akad. Wiss. 424 (1916), https://ui.adsabs.harvard.edu/abs/1916skpa.conf..424S.
[100] R. H. Boyer and R. W. Lindquist, Maximal analytic extension of the Kerr metric, J. Math. Phys. (N.Y.) **8**, 265 (1967).
[101] S. A. Teukolsky, The Kerr metric, Classical Quantum Gravity **32**, 124006 (2015).
[102] A. H. Compton, A quantum theory of the scattering of x-rays by light elements, Phys. Rev. **21**, 483 (1923).
[103] J. D. Bekenstein, Extraction of energy and charge from a black hole, Phys. Rev. D **7**, 949 (1973).
[104] W. E. East and F. Pretorius, Superradiant instability and backreaction of massive vector fields around Kerr black holes, Phys. Rev. Lett. **119**, 041101 (2017).
[105] S. L. Detweiler, Klein-Gordon equation and rotating black holes, Phys. Rev. D **22**, 2323 (1980).
[106] S. R. Dolan, Instability of the massive Klein-Gordon field on the Kerr spacetime, Phys. Rev. D **76**, 084001 (2007).
[107] S. J. Zhu, M. Baryakhtar, M. A. Papa, D. Tsuna, N. Kawanaka, and H.-B. Eggenstein, Characterizing the continuous gravitational-wave signal from boson clouds around galactic isolated black holes, Phys. Rev. D **102**, 063020 (2020).
[108] W. E. East, Massive boson superradiant instability of black holes: Nonlinear growth, saturation, and gravitational radiation, Phys. Rev. Lett. **121**, 131104 (2018).
[109] N. Siemonsen and W. E. East, Gravitational wave signatures of ultralight vector bosons from black hole superradiance, Phys. Rev. D **101**, 024019 (2020).
[110] T. Akutsu *et al.* (KAGRA Collaboration), Overview of KAGRA: Detector design and construction history, Prog. Theor. Exp. Phys. **2021**, 05A101 (2021).
[111] Y. Aso, Y. Michimura, K. Somiya, M. Ando, O. Miyakawa, T. Sekiguchi, D. Tatsumi, and H. Yamamoto, Interferometer design of the KAGRA gravitational wave detector, Phys. Rev. D **88**, 043007 (2013).
[112] B. Iyer, T. Souradeep, C. S. Unnikrishnan, S. Dhuranhar, S. Raja, and A. Sengupta, LIGO-India, proposal of the consortium for Indian initiative in gravitational-wave observations (IndIGO), LIGO Document No. M1100296-v2, 2011.
[113] C. S. Unnikrishnan, IndIGO and LIGO-India: Scope and plans for gravitational wave research and precision metrology in India, Int. J. Mod. Phys. D **22**, 1341010 (2013).
[114] LIGO Scientific Collaboration, Updated advanced LIGO sensitivity design curve, LIGO Document No. T1800044-v5, 2018.
[115] M. Evans, R. X. Adhikari, C. Afle, S. W. Ballmer, S. Biscoveanu, S. Borhanian *et al.*, A horizon study for Cosmic Explorer: Science, observatories, and community, arXiv:2109.09882.
[116] D. Reitze, R. X. Adhikari, S. Ballmer, B. Barish, L. Barsotti, G. Billingsley *et al.*, Cosmic Explorer: The US contribution to gravitational-wave astronomy beyond LIGO, arXiv:1907.04833.
[117] B. P. Abbott, R. Abbott, T. D. Abbott, M. R. Abernathy, K. Ackley, C. Adams *et al.*, Exploring the sensitivity of next generation gravitational wave detectors, Classical Quantum Gravity **34**, 044001 (2017).
[118] A. R. A. C. Wierda, E. Wempe, O. A. Hannuksela, L. V. E. Koopmans, and C. Van Den Broeck, Beyond the detector horizon: Forecasting gravitational-wave strong lensing, Astrophys. J. **921**, 154 (2021).
[119] F. Santoliquido, M. Mapelli, N. Giacobbo, Y. Bouffanais, and M. C. Artale, The cosmic merger rate density of compact objects: Impact of star formation, metallicity,

initial mass function, and binary evolution, Mon. Not. R. Astron. Soc. **502**, 4877 (2021).

[120] B. Abbott, R. Abbott, T. Abbott, M. Abernathy, F. Acernese, K. Ackley *et al.*, Observation of gravitational waves from a binary black hole merger, Phys. Rev. Lett. **116**, 061102 (2016).

[121] B. Abbott, R. Abbott, T. Abbott, S. Abraham, F. Acernese, K. Ackley *et al.*, GWTC-1: A gravitational-wave transient catalog of compact binary mergers observed by LIGO and Virgo during the first and second observing runs, Phys. Rev. X **9**, 031040 (2019).

[122] LIGO Scientific Collaboration, LIGO Algorithm Library—LALSuiteX, free software (GPL), 2018, 10.7935/GT1W-FZ16.

[123] G. Ashton, M. Hübner, P. D. Lasky, C. Talbot, K. Ackley, S. Biscoveanu *et al.*, Bilby: A user-friendly Bayesian inference library for gravitational-wave astronomy, Astrophys. J. Suppl. Ser. **241**, 27 (2019).

[124] J. D. E. Creighton and W. G. Anderson, Gravitational-wave data analysis, in *Gravitational-Wave Physics and Astronomy: An Introduction to Theory, Experiment and Data Analysis* (John Wiley & Sons, Ltd, New York, 2011), pp. 269–347, https://doi.org/10.1002/9783527636037.ch7.

[125] K. Haris, A. K. Mehta, S. Kumar, T. Venumadhav, and P. Ajith, Identifying strongly lensed gravitational wave signals from binary black hole mergers, arXiv:1807.07062.

[126] D. Jones *et al.*, Methods and prospects for gravitational-wave searches targeting ultralight vector-boson clouds around known black holes, Phys. Rev. D **108**, 064001 (2023).

[127] J. D. Hunter, Matplotlib: A 2d graphics environment, Comput. Sci. Eng. **9**, 90 (2007).

[128] C. R. Harris, K. J. Millman, S. J. van der Walt, R. Gommers, P. Virtanen, D. Cournapeau *et al.*, Array programming with NumPy, Nature (London) **585**, 357 (2020).

[129] P. Virtanen, R. Gommers, T. E. Oliphant, M. Haberland, T. Reddy, D. Cournapeau *et al.*, SciPy 1.0: Fundamental algorithms for scientific computing in Python, Nat. Methods **17**, 261 (2020).

[130] F. Pedregosa, G. Varoquaux, A. Gramfort, V. Michel, B. Thirion, O. Grisel, M. Blondel, P. Prettenhofer, R. Weiss, V. Dubourg, J. Vanderplas, A. Passos, D. Cournapeau, M. Brucher, M. Perrot, and É. Duchesnay, Scikit-learn: Machine learning in Python, J. Mach. Learn. Res. **12**, 2825 (2011).

[131] A. Nitz, I. Harry, D. Brown, C. M. Biwer, J. Willis, T. D. Canton *et al.*, GWASTRO/PyCBC, Zenodo v2.3.2, 10.5281/zenodo.10137381 (2023).

[132] M. Vallisneri, Use and abuse of the Fisher information matrix in the assessment of gravitational-wave parameter-estimation prospects, Phys. Rev. D **77**, 042001 (2008).